Journal of Power Sources 226 (2013) 33–41

Contents lists available at SciVerse ScienceDirect

Journal of Power Sources

journal homepage: www.elsevier.com/locate/jpowsour

$LiFePO_4$ battery pack capacity estimation for electric vehicles based on charging cell voltage curve transformation

Yuejiu Zheng, Languang Lu, Xuebing Han, Jianqiu Li, Minggao Ouyang*

State Key Laboratory of Automotive Safety and Energy, Tsinghua University, Beijing 100084, PR China

HIGHLIGHTS

- The uniform charging cell voltage curves (CCVC) hypothesis is proposed.
- Cell capacities can be estimated by overlapping CCVCs using CCVC transformation.
- A simplified approach using voltage-capacity rate curve (VCRC) is proposed.
- Genetic Algorithm (GA) is implemented to find the optimum transformation parameter.
- The battery pack capacity can be precisely estimated with the proposed method.

ARTICLE INFO

Article history:
Received 12 September 2012
Received in revised form
10 October 2012
Accepted 15 October 2012
Available online 29 October 2012

Keywords:
Electric vehicle
Battery pack capacity
Charging cell voltage curves
Cell variations
Genetic algorithm

ABSTRACT

Because of the diversiform driving conditions and the cell variations, it is difficult to accurately determine battery pack capacities in electric vehicles (EVs) by model prediction or direct measurement. This paper studies the charging cell voltage curves (CCVC) for the estimation of the $LiFePO_4$ battery pack capacities in EVs. We propose the uniform CCVC hypothesis and estimate cell capacities by overlapping CCVCs using CCVC transformation. CCVCs of two $LiFePO_4$ cells with large capacity difference are used to verify the hypothesis. We further develop an equivalent simplified approach using voltage-capacity rate curve (VCRC) and implement Genetic Algorithm (GA) to find the optimum transformation parameter for overlapping VCRCs. A small battery pack with four $LiFePO_4$ cells in series is employed to verify the method and the result shows that the estimation errors of both pack capacity and cell capacities are less than 1%. With the proposed method, the battery pack capacity can be precisely estimated which could be used for the driving range prediction. Meanwhile, the estimated cell capacities in battery packs will significantly support the study of cell degradation and cell variations in vehicle driving conditions.

1. Introduction

With rapid progress in power density and energy density increase of the lithium-ion batteries over the past decade, electric vehicles (EVs) with lithium-ion battery packs as power sources have been intensively concerned. However, as one single cell provides insufficient voltage and capacity, it is inevitable to construct battery packs with hundreds of single cells connected in parallel and series to meet the power and energy required in EVs [1,2]. If there were no differences between the cells, we could simply consider the battery pack as one cell with high voltage and large capacity. Current researches on the vehicle level usually adopt this simplified method [3–5]. Unfortunately, due to the inconsistent manufacturing process and the inhomogeneous operating environment, cells always have variations which cannot be eliminated [6,7].

Capacity variations of series-connected cells directly influence the pack capacity. The pack energy density and the driving range of an EV depend on the pack capacity principally. Thus, it is of great significant to estimate the precise pack capacity considering cell capacity variations. The initial pack capacity can be actually calculated through the experiment which is a standard capacity test method recommended by the manufactory. Nevertheless, pack capacity changes as cell capacities fade. As a result, the measured initial pack capacity is meaningless. For electric vehicles, depleting the remaining pack capacity would be good for measuring the pack capacity during operating but it would be a disaster to the driver as nobody is willing to pull his car to the charging station. Research and literature into single cell capacity fade prediction are still the

* Corresponding author. Tel.: +86 10 62792797; fax: +86 10 62789699.
E-mail addresses: yuejiu.zheng@gmail.com (Y. Zheng), ouymg@tsinghua.edu.cn (M. Ouyang).

0378-7753/$ – see front matter
http://dx.doi.org/10.1016/j.jpowsour.2012.10.057

most concerned topics [8–11]. E.V. Thomas et al. [8] and M. Ecker et al. [9] used experimental results of several cells in different conditions to develop the lifetime model. In their experiments, fade rates of cell capacities were different even when cells were in the same test conditions. Therefore, it would be very difficult and inaccurate to predict the pack capacity fade using similar methods that predict single cell capacity. As a consequence, little literature explores prediction methods for pack capacities.

Because it is almost impossible to measure the pack capacity in EVs due to the driving condition and also predicting the pack capacity is inaccurate, precise pack capacity estimation in EVs is a challenging task. Several cell capacity estimation approaches were studied in literature [12–15]. G. L. Plett [12] and H.F. Dai et al. [13] used dual Kalman filtering for state of charge (SOC) and capacity estimation. C. Hu et al. [14] proposed an improved multiscale framework with Kalman filtering for SOC and capacity estimation. The estimation results were satisfactory as accurate battery models for cells were implemented. However, it is difficult to construct an accurate model concerning inconsistent cells in the battery pack. G. L. Plett [15] utilized a total least squares estimation method to estimate cell capacity, and no accurate battery models were involved using this method. K. Honkura et al. [10] analyzed discharge curves to predict capacity fade of lithium-ion batteries. Nevertheless, accurate pack capacity estimation regarding cell variations was not focused in above studies.

This paper first introduces the definition of battery "pack capacity" concerning cell variations in Section 2. And subsequently we associate pack capacity with cell capacities. We propose the uniform charging cell voltage curve (CCVC) hypothesis in Section 3: when internal resistances, initial remaining cell capacities and total cell capacities of cells in one batch are the same, CCVCs of the cells in the pack are the same, which means that voltage–capacity curves are completely overlapped. And we deduce that by CCVC transformation, CCVCs of cells with different internal resistances, initial remaining cell capacities and total cell capacities can be overlapped and cell capacities can be calculated. CCVCs of two $LiFePO_4$ cells with large capacity difference are used to verify the hypothesis and the result shows that the calculated cell capacity is satisfactory. We further develop an equivalent simplified approach using voltage–capacity rate curve (VCRC) transformation. In Section 4, Genetic Algorithm (GA) is implemented to find the optimum transformation parameter. A small battery pack with four $LiFePO_4$ cells in series is employed to verify the method and the result shows that the estimation errors of both pack capacity and cell capacities are qualified. With the proposed method, data of CCVCs can be used to estimate pack capacities in EVs, which is benefit to accurate driving range estimation. In addition, cell capacities calculated in battery packs will support the study of cell degradation and variations in vehicle driving conditions, and the calculated cell capacities are also the key information for cell equalization strategies.

2. Pack capacity and charging cell voltage curves

2.1. Pack capacity

Pack capacity is total available ampere-hours released from a fully charged state of one cell in the battery pack to a fully discharged state of one or other cell at a constant discharge rate of 1/3C at room temperature of 25 °C. Pack capacity is commonly defined by discharging capacity, but regarding high coulombic efficiency of commercial $LiFePO_4$ cells in EVs, difference of charging capacity and discharging capacity is negligible. As discharging process depends on EV's driving condition which is volatile, while the charging process is fixed at a designed charging current, pack charging capacity as pack capacity is satisfactory in EVs.

When one or some cell is fully discharged (marked as Cell A) during discharging without cell equalization, other cells still have some remaining capacities because of the difference in cell capacity and SOC. But the battery pack is not allowed to discharge; otherwise it would greatly reduce the life of the battery pack, or even raise severe safety problems. Similarly, when one or some cell is fully charged (marked as Cell B, and Cell B may be Cell A) during charging, other cells are still not fully charged, but the battery pack is not allowed to charge. The charged capacity during charging process from fully discharged Cell A to fully charged Cell B can be called pack capacity as defined. When Cell B is Cell A, pack capacity is exactly the capacity of Cell A. The releasable capacity of a battery pack is the minimum remaining cell capacity and the absorbable capacity is the minimum capacity that can be charged. Pack capacity then can be considered as the sum of the minimum remaining cell capacity and the minimum capacity that can be charged. This can be formulated as

$$C_{\mathrm{Pack}}(t) = \min(C_{\mathrm{r}}(t)) + \min((1-\mathrm{SOC}(t))\cdot C(t)) \tag{1}$$

where $C_{\mathrm{Pack}}(t)$ is the pack capacity at its lifetime t, $C_{\mathrm{r}}(t)$ is the remaining cell capacity, $\mathrm{SOC}(t)$ is the cell current state of charge and $C(t)$ is the cell capacity. When the cell with the minimum remaining cell capacity has the minimum capacity that can be charged, the pack capacity is equal to the cell capacity, and the capacity of the cell is also the minimum in the battery pack. The cell with the minimum remaining cell capacity does not have the minimum capacity that can be charged in the majority of the battery packs, so pack capacity is usually less than all of the cell capacities in the pack.

For dissipation cell equalization such as resistor shunt equalization, the cell with minimum cell capacity is fully charged and discharged. Thus, pack capacity is the minimum cell capacity,

$$C_{\mathrm{Pack}}(t) = \min(C(t)) \tag{2}$$

For non-dissipation cell equalization [16,17] which transfers the energy from cell to cell at all time, the maximum pack capacity the battery pack may reach is the mean cell capacity,

$$C_{\mathrm{Pack}}(t) = \mathrm{mean}(C(t)) \tag{3}$$

Therefore, the relationship between pack capacity and cell capacities is

$$C_{\mathrm{Pack}}(t) = \begin{cases} \min(C_{\mathrm{r}}(t) + \min((1-\mathrm{SOC}(t)))\cdot C(t)) & \text{without equlization} \\ \min(C(t)) & \text{dissipation equlization} \\ \mathrm{mean}(C(t)) & \text{non}-\text{dissipation equlization} \end{cases} \tag{4}$$

No matter cell equalization is applied or not, statistical cell capacities are needed to calculate pack capacity. However, cell capacities are impossible to be measured in vehicle applications. Even though hundreds of cell capacities were measured before cell grouping, we could just know initial cell capacities and initial pack capacities. As the cell capacity fade rates are different from cell to cell due to the complex thermoelectric conditions in EVs, it is almost impossible to accurately predict every single cell capacities.

2.2. Charging cell voltage curves of $LiFePO_4$

A typical $LiFePO_4$ cell CCVC is shown in Fig. 1. A cell enters charging period after rest in the fully discharged state. A standard CC–CV charging profile is used to charge the cell. The first period is the constant current charging period (CC period). The cell is charged at 1/3C constant current until the charge cutoff voltage which is 3.6 V for $LiFePO_4$ cell as recommended. After CC charging, the cell experienced a constant voltage charging period (CV period) until current reaches the cutoff current which is 1/20C. The charged capacity is divided into two parts according to the charging periods, CC capacity and CV capacity. Under the standard charging profile, CV capacity accounts for approximately 2% of cell capacity (see Section 4.1). As the CV control technology of single cells in the pack is relatively complex, many EVs prefer charging without CV period.

Fig. 2 shows CCVCs of a battery pack composed of four $LiFePO_4$ cells in series with a nominal capacity of 6.5 A h. The pack starts charging at a constant current of 2.16 A which is 1/3C from the fully discharged state of Cell 2, and stops when Cell 4 reaches the charge cutoff voltage of 3.6 V. Generally, CCVCs are close to each other in Fig. 2. Details of Fig. 2 in the blue dotted and brown solid boxes show that only Cell 2 is at its fully discharge state before charging and only Cell 4 is charged to the charge cutoff voltage. We can deduce that Cell 2 has the minimum remaining capacity when discharged and Cell 4 has the minimum absorbable capacity when charged. Thus, the pack capacity is less than all of the 4 cell capacities. We can calculate pack capacity according to Formula (1). As the pack starts charging from the fully discharged state and ends at the fully charged state, the pack capacity can be calculated directly (For interpretation of the references to colour in this figure legend, the reader is referred to the web version of this article.).

Compared to the complete charging in Fig. 2 which normally happens in the laboratory, CCVCs in EVs are always incomplete. This is because drivers always charge the packs before they are empty, and they prefer battery packs in the fully charged state. It means CCVCs in EVs never start at the fully discharged state but usually end at the fully charged state. Fig. 3 shows CCVCs of the same pack in Fig. 2 that simulates possible CCVCs of battery packs

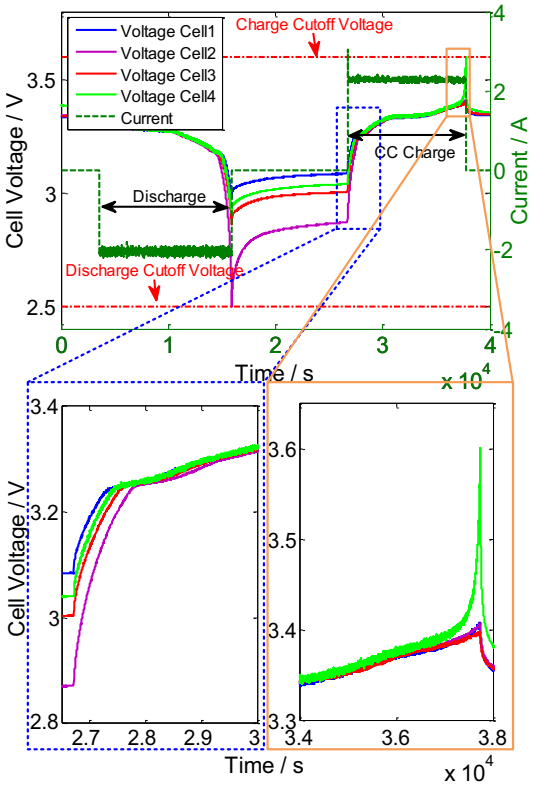

Fig. 2. CCVCs of a battery pack with four $LiFePO_4$ cells in series.

installed in EVs. The pack starts charging when none of the cells are fully discharged and ends when Cell 4 reaches the charge cutoff voltage. In this case, the pack capacity is no longer measurable using ampere-hour integral.

As Cell 4 reaches the charge cutoff voltage before other cells, we manually discharge Cell 4 slightly. Fig. 4 displays CCVCs after cell equalization. Details of Fig. 4 in the blue dotted and brown solid boxes show that Cell 4 reaches the discharge cutoff voltage together with Cell 2 when fully discharged, and the pack still stops charging when Cell 4 reaches charge cutoff voltage. This indicates a cell capacity difference between Cell 2 and 4. We also infer that Cell 4 has a minimum cell capacity. Since Cell 4 can be fully charged and discharged in the pack, the pack capacity is equal to Cell 4. For Cell 1 and 3, although they have remaining capacities when Cell 4 is fully discharged, they do not reach the charge cutoff voltage when Cell 4

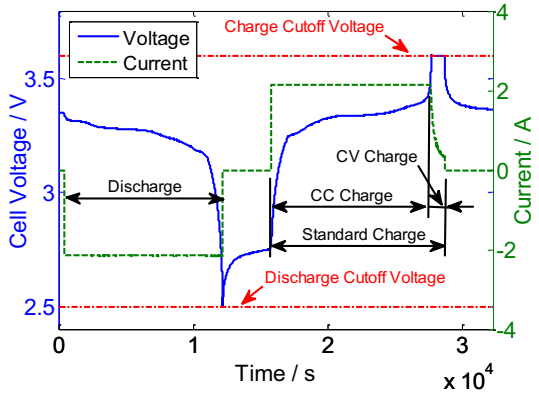

Fig. 1. A typical $LiFePO_4$ cell CCVC.

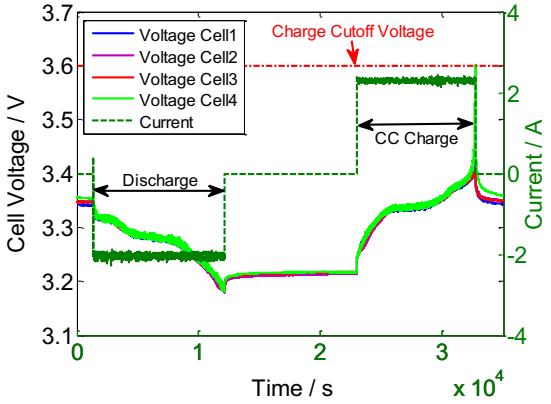

Fig. 3. Incomplete CCVCs of the battery pack.

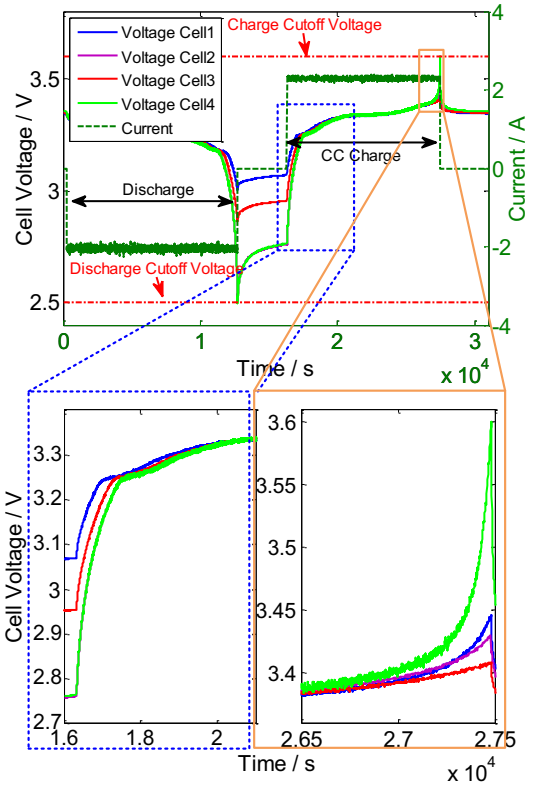

Fig. 4. Complete CCVCs after cell equalization.

is fully charged. They will not constrain the battery pack capacity, and no equalization is required for Cell 1 and 3 (For interpretation of the references to colour in this figure legend, the reader is referred to the web version of this article.).

3. Uniform CCVC hypothesis and preliminary validation

3.1. Uniform CCVC hypothesis

The relationship between OCV and SOC of $LiFePO_4$ is unvaried [18,19] as OCV is the external performance of the cell electrochemical equilibrium state. For cells of the same type, SOC–OCV curves are uniform. CCVC and OCV curves of a $LiFePO_4$ cell are compared in Fig. 5. CCVC is very close to OCV except at the end of the charging process where CCVC raises to a high level due to charging polarization. The difference between charging cell voltage and OCV is the overpotential, and it can be divided into three categories, namely activation overpotential η_a, concentration overpotential η_c and resistance overpotential η_r.

According to Butler–Volmer equation

$$I = A \cdot i_0 \cdot \left\{ \exp\left[\frac{\alpha_a nF}{RT}\eta_a\right] - \exp\left[-\frac{\alpha_c nF}{RT}\eta_a\right] \right\} \quad (5)$$

where

I: electrode current
A: electrode active surface area
i_0: exchange current density
R: universal gas constant
T: absolute temperature
n: number of electrons involved in the electrode reaction
F: Faraday constant
α_c: cathodic charge transfer coefficient
α_a: anodic charge transfer coefficient
η_a: activation overpotential

If the charging environment is the same which means current and temperature of the cells are the same, and if SOCs of the cells are the same which means the exchange current density i_0 and electrodynamics potential E_{eq} (OCV) of the cells are the same, the activation overpotential η_a depends on the electrode active surface area A, cathodic charge transfer coefficient α_c and anodic charge transfer coefficient α_a. As the electrode active surface area of cells in the same batch are very close to each other and $\alpha_a = \alpha_c = 0.5$ for most reactions, activation overpotential with the same is approximately the same from cell to cell.

Regarding concentration overpotential η_c, according to equation

$$\eta_c = \frac{RT}{nF}\ln(C_B/C_E) \quad (6)$$

where C_B is bulk concentration and C_E is electrode concentration. When cells are charged with the same SOC, differences of the concentration are small. Therefore the concentration overpotential η_c is also similar from cell to cell. And for resistance overpotential η_r, if the cell ohmic resistances are the same, resistance overpotentials η_r are the same.

We therefore hypothesize that in a battery pack with cells of one batch, if internal resistances, initial remaining cell capacities and total cell capacities are the same, CCVCs of the cells are the same,

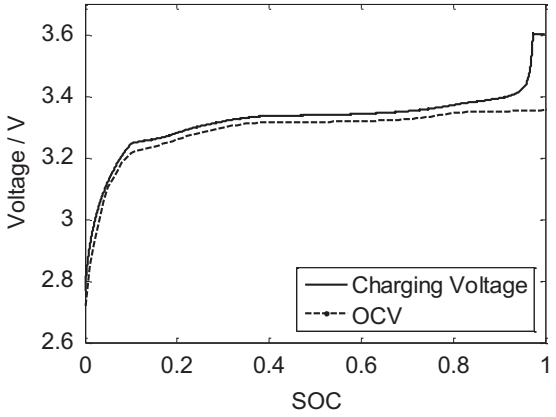

Fig. 5. Comparison of CCVC and OCV curves of a $LiFePO_4$ cell.

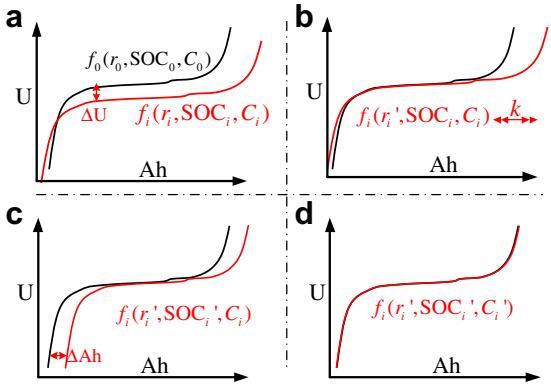

Fig. 6. Schematic diagram of CCVC overlapping procedures.

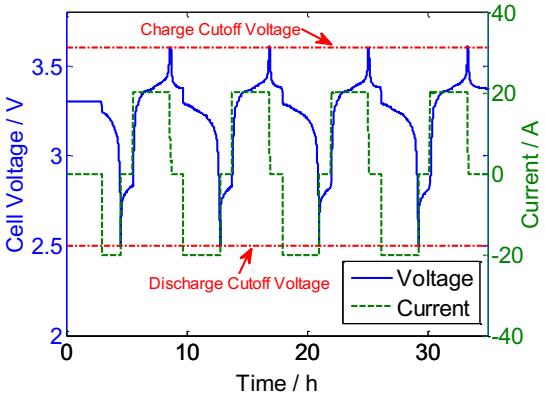

Fig. 7. Current profile and CCVC of the standard capacity test for Cell A.

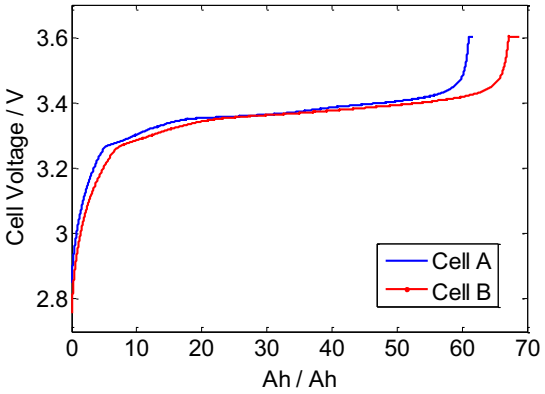

Fig. 8. CCVCs of two $LiFePO_4$ cells with the horizontal axis of ampere-hours.

which means that voltage–capacity curves are completely overlapped. We also deduce that by CCVC transformation, CCVCs of cells with different internal resistances, initial remaining cell capacities and total cell capacities can be overlapped and cell capacities can be calculated. Different internal resistances are eliminated by CCVC vertical translations, different initial remaining cell capacities are compensated by CCVC horizontal translations and by horizontal scaling, influence of different cell capacities to CCVCs are eliminated.

Detail procedures are demonstrated in Fig. 6. We assume CCVC of Cell 0 is known as f_0, and its internal resistance r_0, initial SOC_0 and cell capacity C_0 are also known. CCVC of Cell i is known as f_i, but its internal resistance r_i, initial SOC_i and cell capacity C_i are unknown. Original CCVCs are shown in Fig. 6(a). By CCVC vertical translation ΔU, we get Fig. 6(b), and Fig. 6(c) is achieved by horizontal scaling k. Finally, by horizontal translation, f_i is overlapped with f_0 in Fig. 6(d). The internal resistance r_i, initial SOC_i and cell capacity C_i can be calculated using Formula (7)

$$\begin{aligned} r_i &= r_0 + \frac{\Delta U}{I} \\ C_i &= kC_0 \\ SOC_i &= SOC_0 + \frac{\Delta Ah}{C_0} \end{aligned} \tag{7}$$

$\Delta U > 0$, if f_i moves downward and $\Delta U < 0$ if f_i moves upward; $k > 1$ if f_i zooms out and $k < 1$ if f_i zooms in; $\Delta Ah < 0$, if f_i moves left and $\Delta Ah > 0$ if f_i moves right.

3.2. Preliminary experimental validation

Two commercial $LiFePO_4$ cells of one type but with different capacities of 60 A h (Cell A) and 70 A h (Cell B) are selected to preliminary verify the uniform CCVC hypothesis. Standard capacity tests are used to test cell capacities, and also CCVCs are achieved during the test. Current profile and CCVC of the standard capacity test for Cell A are depicted in Fig. 7. The cell is charged at the constant current of 1/3C (20 A) after it reaches the discharge cutoff voltage 2.5 V. The charging process changes from CC to CV when cell voltage reaches charge cutoff voltage 3.6 V, and stops when the charge cutoff current of 1/20C (3 A) is reached. After that, the cell is ready for the standard capacity test. And the cell is then cycled for 3 times at standard capacity test current profile. Ampere-hour integral method is used to calculate the average capacity of the 3 cycles for the cell capacity.

Cell B is tested with the same method. And the capacities of the two cells are listed in Table 1. Total charge capacity is the sum of the CC charge capacity and CV charge capacity. The cell capacities are 61.57 A h and 68.61 A h respectively regarding the discharge capacities. As the total charge capacities are close to the discharge capacities, the error is less than 0.2% when total charge capacities are used to represent the cell capacities.

Fig. 8 shows CCVCs in one complete standard charging cycle of the two cells with the horizontal axis of ampere-hours. The curves are not overlapped due to the different cell capacities.

We assume that capacity of Cell A is known, and thus CCVC of Cell A (f_a) is the standard CCVC. By curve transformation, we try to overlap CCVC of Cell B (f_b) with f_a. f_a and the transformed curve of f_b are shown in Fig. 9, and the transformation parameters achieved by trial and error method are $\Delta U = 0$, $k = 1.095$, $\Delta Ah = -0.5$ A h. Better parameters are possible, but the achieved parameters are good to overlap the CCVCs. We use Formula (7) to calculate the capacity and initial SOC of Cell B. The results are compared in Table 2. The capacity estimation errors are less than 2% and initial SOC error less than 1%. The result shows that it is feasible to estimate cell capacities by curve transformation, and also the uniform CCVC hypothesis is reliable.

Table 1
Capacities of two commercial $LiFePO_4$ cells.

Cell type	Cell A	Cell B
Discharge capacity (A h)	61.57	68.61
CC charge capacity (A h)	60.55	67.17
CV charge capacity (A h)	1.17	1.62
Total charge capacity (A h)	61.72	68.79

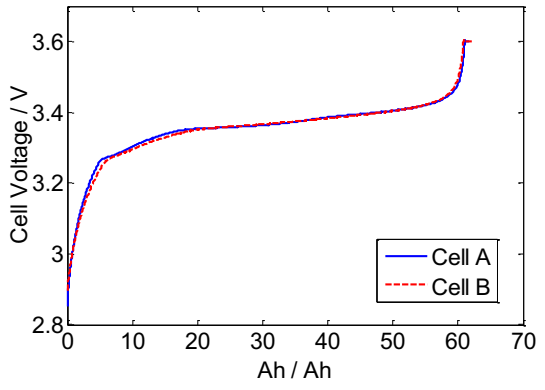

Fig. 9. CCVC of Cell A and transformed CCVC of Cell B.

Table 2
Cell capacity and initial SOC estimation errors by curve transformation.

Cell type	Cell A	Cell B (estimated)	Cell B (measured)	Difference/ accuracy
CC charge capacity (A h)	60.55	66.30	67.17	0.87/1.30%
Total charge capacity (A h)	61.72	67.58	68.79	1.21/1.76%
Initial SOC	0	−0.8%	0	0.8%

The main purpose of this paper is to estimate the pack capacity and cell capacity, so internal resistances are not concerned in this study. It is better to reduce the three-dimensional problem (ΔU, ΔAh and k) to two-dimensional problem (ΔAh and k). The slope of CCVC is not influenced by CCVC vertical translation, and it is independent of parameter ΔU. We use the parameters ΔAh and k to overlap the slope curve of CCVC which is called as voltage–capacity rate curve (VCRC) in this paper for convenience. The voltage–capacity rate stands for the voltage increase in an ampere-hour. Fig. 10 shows VCRCs of cells, the CCVCs of which are plotted in Fig. 8. As expected, VCRCs are similar. With horizontal translation ΔAh, horizontal contraction k and vertical expansion k, VCRCs will overlap.

As we fully charge and discharge the cells, the initial SOCs of the cells are the same. So we do not need to focus on the initial SOC in our preliminary experimental validation and no horizontal translation is required. Horizontal contraction k and vertical expansion k are applied to transform VCRC of Cell B. Fig. 11 demonstrates comparison of the transformed VCRCs of Cell B at different contraction/expansion k with VCRC of Cell A. when $k = 1.1$, the transformed VCRC of Cell B is very close to VCRC of Cell A. The blue dashed box shows that when $k = 1.095$ or $k = 1.105$, the transformed VCRCs of Cell B are not as good as when $k = 1.1$. We conclude that $k = 1.1$ is a better solution, and the corresponding calculated CC charge capacity of Cell B is 66.61 A h, which is 0.56 A h less than the measured capacity. The relative error is less than 1% (For interpretation of the references to colour in this figure legend, the reader is referred to the web version of this article.).

The accuracy of the cell capacity estimation by CCVC/VCRC transformation is proved to be satisfactory. However, it is subjective by observing the overlapped CCVC/VCRC and the trial and error method also causes a lot of time, so it cannot be applied in EVs for cell capacity estimation. In addition, CCVCs of the two cells are achieved respectively and completely, but CCVCs in EVs are usually not complete and errors of the estimated cell capacities and pack capacity are still to be verified.

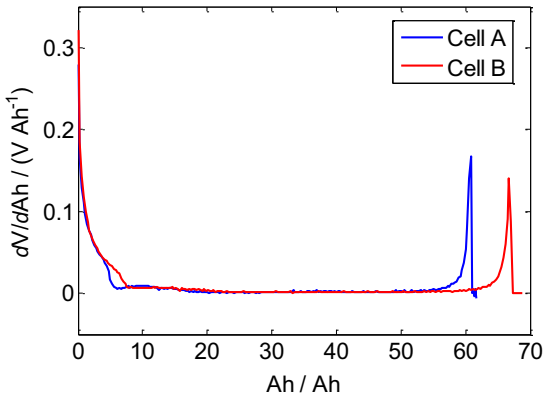

Fig. 10. Slope curves of CCVCs of the 2 $LiFePO_4$ cells (VCRCs).

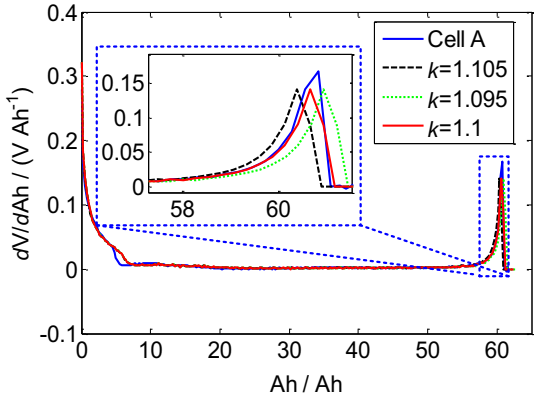

Fig. 11. VCRC of Cell A and the transformed VCRCs of Cell B with different transformation parameter k.

4. Pack capacity estimation

4.1. Charging experiment of a battery pack

A small battery pack consists of four $LiFePO_4$ cells in series with a nominal capacity of 6.5 A h is employed to simulate possible CCVCs of battery packs installed in EVs. Cell capacities are tested before grouped, and one of the cell capacity test profile is shown in Fig. 1. The cell capacities are listed in Table 3. The maximum capacity of the four cells is Cell 3, and the minimum capacity Cell 4. The CC charge capacity is approximately 98% of the total charge capacity. The cells are at the fully charged state after the standard capacity test. But in order to simulate different SOCs in the pack, the initial remaining capacities are conditioned at a discharge current of 3 A. The cells are discharged for 5, 6, 9 and 0 min with 0.25, 0.3, 0.45 and 0 A h released from the respective cells. The condition can be arbitrary as SOCs in the pack are various. The conditioned initial remaining capacities are also listed in Table 3.

After cell capacity test and conditioning, the cells are connected in series for a complete pack charging in Fig. 2. As the initial remaining capacity of Cell 2 is the minimum, it reaches the discharge cutoff voltage before other cells. Cell 4 reaches the charge cutoff voltage before others as it has the minimum absorbable capacity. We can directly calculate the pack capacity by ampere-hour method as the pack has a complete charge. The pack capacity is 7.033 A h, which is less than any cell capacities as expected.

As CCVCs in EVs never start at the fully discharged state but usually end at the fully charged state, we further simulate possible CCVCs of battery packs installed in EVs in Fig. 3. The pack starts charging when none of the cells are fully discharged and ends when Cell 4 reaches the charge cutoff voltage. The charged ampere-hours of 6.226 A h is no longer the pack capacity.

Due to the unknown cell capacities, cell SOC estimation by ampere-hour method is inaccurate, but cell SOC estimation by SOC–OCV curve does not depend on cell capacities. The SOC–OCV curve of the $LiFePO_4$ is plotted in Fig. 12. Probability density distribution of OCVs is drawn along the vertical axis. As can be seen,

Table 3
Cell capacities and initial remaining capacity of 4 $LiFePO_4$ cells.

Cell	Cell #1	Cell #2	Cell #3	Cell #4
Total charge capacity (A h)	7.6085	7.4494	7.6684	7.2831
CC charge capacity (A h)	7.4464	7.2934	7.5191	7.1171
Initial remaining capacity (A h)	7.3585	7.1494	7.2184	7.2831

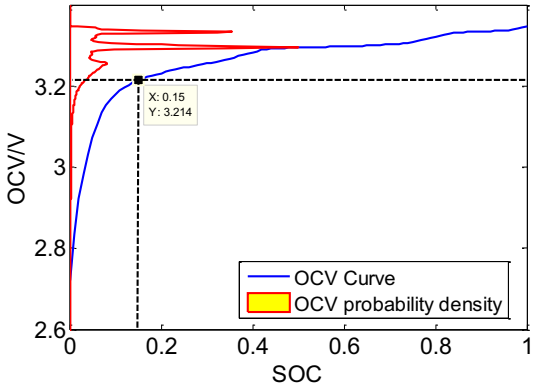

Fig. 12. SOC–OCV curve of the $LiFePO_4$ Cell and the probability density distribution of OCVs.

when SOC is less than 15% and the voltage is less 3.214 V, the OCV probability density is small which means that the accuracy of the estimated SOC is high when the measured OCV is less than 3.214 V. But if the measured OCV is larger than 3.214 V, the OCV probability density is large and its corresponding SOC interval is large which means the accuracy of the estimated SOC is not reliable.

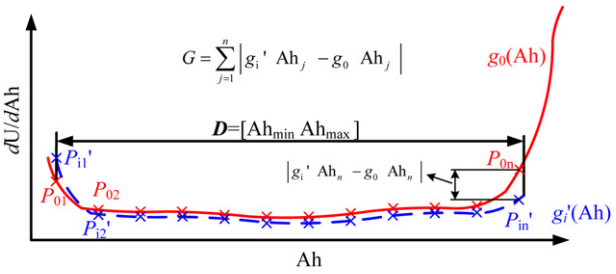

Fig. 13. Objective function construction for VCRC transformation.

The cell capacity of VCRC $g_0(\mathrm{Ah})$ is already known. The objective is to determine the best transformation parameter $\boldsymbol{T} = [k, \Delta\mathrm{Ah}]$ to make VCRC transformation from VCRC $g_i(\mathrm{Ah})$ to VCRC $g_i'(\mathrm{Ah}) = kg_i(Ah/k - \Delta\mathrm{Ah})$ so as to overlap VCRC $g_i'(\mathrm{Ah})$ and VCRC $g_0(\mathrm{Ah})$. As demonstrated in Fig. 13, an approximate method for the best curve overlapping is to minimize the distances of the corresponding points on the curves. The coincident domain of $g_0(\mathrm{Ah})$ and $g_i'(\mathrm{Ah})$ is denoted as $\boldsymbol{D} = [\mathrm{Ah}_{\min}\ \mathrm{Ah}_{\max}]$. Corresponding points are chosen every certain ampere-hour, e.g. $(\mathrm{Ah}_{\max} - \mathrm{Ah}_{\min})/50$. These points are marked as follows:

$$P_0 = \{P_{01}, P_{02}, \ldots P_{0n}\} = \{(\mathrm{Ah}_1, g_0(\mathrm{Ah}_1)), (\mathrm{Ah}_2, g_0(\mathrm{Ah}_2)), \ldots (\mathrm{Ah}_n, g_0(\mathrm{Ah}_n))\};$$
$$P_i' = \{P_{i1}', P_{i2}', \ldots P_{in}'\} = \{(\mathrm{Ah}_1, g_i'(\mathrm{Ah}_1)), (\mathrm{Ah}_2, g_i'(\mathrm{Ah}_2)), \ldots (\mathrm{Ah}_n, g_i'(\mathrm{Ah}_n))\};$$
$$\mathrm{Ah}_1,\ \mathrm{Ah}_2 \ldots \mathrm{Ah}_n, \in D$$

Before the incomplete charging shown in Fig. 3, the battery pack rests for 3 h to achieve cell OCVs. All the measured OCVs are less than 3.21 V, and accurate SOCs can be achieved by SOC–OCV curve in Table 4. As Cell 4 reaches the charge cutoff voltage, the SOC is 100% when the pack is fully charged. Capacity of Cell 4 then can be calculated: 6.226 A h/(100%–13.2%) = 7.17 A h. Compared to the measured capacity, the calculated capacity of Cell 4 is 0.05 A h larger. The error is less than 1%.

However, only capacity of Cell 4 can be calculated, because it is the only cell that is fully charged. For other three cells, SOCs are indeterminate at the end of charging, so the capacities cannot be calculated as Cell 4.

The estimated capacity of Cell 4 is the foundation for capacity estimation of the other cells. With the known capacity of Cell 4, CCVC transformation can be applied to the other cells. Capacities of these cells as well as the pack capacity can be estimated.

4.2. Pack capacity estimation by genetic algorithm

We have verified that VCRC transformation is reliable for cell capacity estimation. But we need to seek a better mathematical solution as the trial and error method is ineffectiveness.

The objective function is constructed in Eq. (8)

$$G = \sum_{j=1}^{n} |g_i'(\mathrm{Ah}_j) - g_0(\mathrm{Ah}_j)| \tag{8}$$

Theoretically when the best transformation parameter $\boldsymbol{T} = [k, \Delta\mathrm{Ah}]$ is applied to VCRC g_i, g_i' is overlapped with VCRC g_0. As a result, $\boldsymbol{P}_0$ and $\boldsymbol{P}_i'$ are the same, so the objective function $G = G_{\min,\mathrm{global}} = 0$ is the global minimum. As the voltage measurement error always exists, there is no doubt that g_i' cannot completely match VCRC g_0 no matter what transformation parameter $\boldsymbol{T}$ is applied. But if the objective function G reaches its minimum value, g_i' matches VCRC g_0 in the maximal degree. The transformation parameter $\boldsymbol{T}$ is then considered suitable for VCRC transformation. We can get the cell capacity and its SOC corresponding to VCRC g_i using Formula (7) with $\boldsymbol{T} = [k, \Delta\mathrm{Ah}]$ substituted.

The transformation parameter $\boldsymbol{T} = [k, \Delta\mathrm{Ah}]$ can be determined by some global optimization methods. Because the objective function G is not continuously differentiable, it is difficult to utilize the traditional optimization methods. Though the exhaustive method is a possible approach, it is lack of efficiency. Holland and

Table 4
Cell SOCs before charging and the determined cell capacity.

Cell	Cell #1	Cell #2	Cell #3	Cell #4	Pack
Measured CC charge capacity (A h)	7.4464	7.2934	7.5191	7.1171	7.033
Initial SOC (%)	13.6	11.1	11.7	13.2	–
Calculated CC charge capacity (A h)	–	–	–	7.17	–

Table 5
Settings in Matlab® GA toolbox.

Parameter	Value
Fitness function	Formula (8)
Number of variables	2
Bounds	$k \in [0.8\ 1.2]$, $\Delta\mathrm{Ah} \in [-1\ 1]$
Population size	100
Number of generations	100
Selection function	Stochastic uniform
Crossover fraction	0.8
Mutation function	Adaptive feasible

Table 6
Estimated cell capacities and SOCs by GA and their errors.

Cell	Cell #1	Cell #2	Cell #3
K	1.044	1.021	1.052
Calculated CC charge capacity (A h)	7.49	7.32	7.54
Measured CC charge capacity (A h)	7.4464	7.2934	7.5191
Capacity estimation error (%)	0.59	0.36	0.28
ΔAh (A h)	−0.011	−0.124	−0.090
Calculated SOC (%)	13.06	11.47	11.95
Measured SOC (%)	13.6	11.1	11.7
SOC estimation error (%)	0.54	0.37	0.25

Table 7
The estimated pack capacity and its error.

Cell	Cell #1	Cell #2	Cell #3	Cell #4
C_r (A h)	0.98	**0.84**	0.90	0.95
$(1 - SOC)\bullet C$ (A h)	6.51	6.48	6.64	**6.22**
$\min(C_r(t))$ (A h)	0.84			
$\min((1 - SOC(t))\bullet C(t))$ (A h)	6.22			
Calculated C_{Pack} (A h)	7.06			
Measured C_{Pack} (A h)	7.033			
C_{Pack} estimation error (%)	0.4			

Bold value indicates they are the smallest numbers of each rows.

his students in the University of Michigan, USA, proposed the Genetic Algorithm (GA) which is an efficient and strong robust global optimization algorithm. It can quickly and reliably solve problems with complex objective functions which are not continuously differentiable [20]. GA is employed to search the global optimization transformation parameter $\boldsymbol{T}$ in this paper.

GA is based on natural selection which is completely different from the traditional optimization methods. GA simulates natural biological evolution according to the "fitness level" of the individuals which are a large set of possible solutions to a given problem. Through the genetic operators (selection, crossover, and mutation) and natural selection, better generations are bred. By selection operator, parent solutions which have better fitness level are more likely to reproduce which means better genes are more likely to dominate the next generation. Crossover combines the features of two parents at a certain crossover fraction to form new solutions by swapping corresponding segments of parent chromosomes. By randomly changing one or more genes at a low mutation rate, mutation introduces variability into the next generation that will stop GA converging at a local minimum.

Matlab® GA toolbox is employed to resolve the global optimization VCRC transformation parameter $\boldsymbol{T}$ in this paper. The parameters for the VCRC transformation are listed in Table 5. The fitness function is the objective function in Eq. (8). In the Matlab® GA toolbox, a smaller fitness function value means a better fitness level. As a result, the best individual of all the generations is the best transformation parameter to minimize the objective function G. We have 2 variables in the transformation parameter $\boldsymbol{T}$. Their bounds are set $k \in [0.8\ 1.2]$, $\Delta Ah \in [-1\ 1]$, because the differences of cell capacities and SOCs will not exceed 20% normally when there are no faults occurred in the pack. 100 generations are bred and the population size is 100 for each generation. Selection function uses stochastic uniform algorithm which ensures that the fitness levels of the parent individuals are corresponding to their selection probability. Mutation function uses adaptive feasible algorithm which generates mutation direction randomly and selects the mutation step length in the range of the transformation parameter bounds.

Transformation parameters of VCRCs for Cell 1, 2 and 3 are optimized by GA and the results are shown in Table 6. The capacity and SOC estimation errors are all well below 1% which indicates that GA is considerably effective for parameter optimization of VCRC transformation.

Take Cell 1 for example, the transformation parameter $\boldsymbol{T} = [1.044\ -0.011]$, i.e. $k = 1.044$, $\Delta Ah = -0.011$. According to Formula (7), the estimated cell capacity is 7.49 A h with an error of 0.59% and the estimated SOC is 13.06% with an error of 0.54%. Fig. 14 depicts VCRC and CCVC of Cell 1 before and after curve transformation. VCRC and CCVC of Cell 4 are also plotted in Fig. 14 using the red solid curves. The blue dashed curves are VCRC and CCVC before transformation, and after transformation they turn to blue solid curves. As can be seen, the transformed VCRC and CCVC of Cell 1 are well overlapped with those of Cell 4 in the figure (For interpretation of the references to colour in this figure legend, the reader is referred to the web version of this article.).

Formula (1) is applied to calculate the pack capacity based on the results of cell capacities and SOCs. The estimated pack capacity is shown in Table 7. As expected in Section 2.2, Cell 2 has the least ampere-hours that can be released and Cell 4 has the least ampere-hours that can be charged. The estimated pack capacity is 7.06 A h with an error of 0.4% compared to the measured pack capacity 7.033 A h.

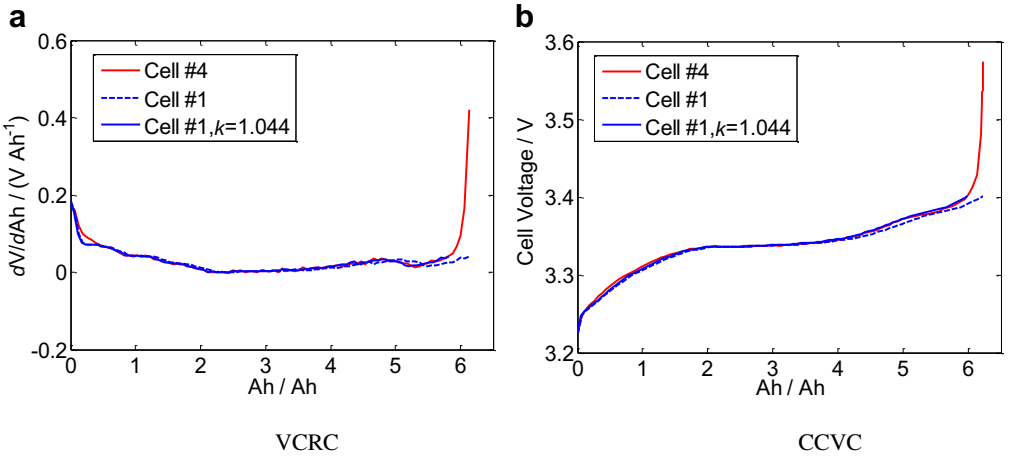

Fig. 14. The comparison of VCRC and CCVC of Cell 4 and those of Cell 1 before and after curve transformation.

5. Conclusion

An accurate estimation of the battery pack capacity is significant for forecasting the EV driving range. But because of the diversiform driving conditions and the cell variations, it is difficult to accurately determine battery pack capacities in EVs by model prediction or direct measurement. This paper studies CCVC and VCRC transformation for the estimation of the $LiFePO_4$ battery pack capacities in EVs.

Firstly, we believe that with cell variations taking into consideration the pack capacity is different from the cell capacities in the pack. Thus we deduce the quantitative relationship between pack capacities and cell capacities in the packs.

Secondly, we propose the uniform CCVC hypothesis that in a battery pack with cells of one batch, if internal resistances, initial remaining cell capacities and total cell capacities are the same, CCVCs of the cells are the same. We estimate cell capacities by overlapping the CCVCs using CCVC transformation. CCVCs of two $LiFePO_4$ cells with large capacity difference are used to verify the hypothesis and the result shows a satisfactory accuracy of cell estimation.

Finally, we further develop an equivalent simplified approach using VCRC and implement GA to find the optimum transformation parameter for overlapping VCRCs. A small battery pack with four $LiFePO_4$ cells in series is employed to verify the method and the result shows that the estimation errors of both pack capacity and cell capacities are less than 1%.

With the proposed method and easily achieved CCVCs in EVs, the pack capacity can be precisely estimated. In addition, cell capacities calculated in battery packs will support the study of cell degradation and variations in vehicle driving conditions, and the calculated cell capacities are also the key information for cell equalization strategies.

Further studies are to be carried on in the following three aspects. First, more CCVCs in EVs are encouraged to prove the uniform CCVC hypothesis as the authors have limited data; Second, cells of other types, e.g. $LiMnO_4$, are to be studied besides $LiFePO_4$ cells to discover whether the uniform CCVC hypothesis is suitable for other cells; Third, more simple algorithms are to be developed for on line estimation of cell capacities and pack capacities in EVs as GA is still complex in computing for vehicle applications.

Acknowledgement

This research is funded by the MOST (Ministry of Science and Technology) of China under the contract of No.2010DFA72760 and the Tsinghua University Initiative Scientific Research Program (Grand No. 2010THZ08116).

References

[1] G.J. Offer, V. Yufit, D.A. Howey, B. Wu, N.P. Brandon, J. Power Sources 206 (2012) 383–392.
[2] M.S. Wu, C.Y. Lin, Y.Y. Wang, C.C. Wan, C.R. Yang, Electrochim. Acta 52 (2006) 1349–1357.
[3] X.J. Li, J.Q. Li, L.F. Xu, M.G. Ouyang, X.B. Han, L.G. Lu, C.T. Lin, J. Power Sources 195 (2010) 3338–3343.
[4] F.C. Sun, X.S. Hu, Y. Zou, S.G. Li, Energy 36 (2011) 3531–3540.
[5] E. Wooda, M. Alexanderb, T.H. Bradley, J. Power Sources 196 (2011) 5147–5154.
[6] B. Kenney, K. Darcovich, D.D. MacNeil, I.J. Davidson, J. Power Sources 213 (2012) 391–401.
[7] M. Dubarry, C. Truchot, M. Cugnet, B.Y. Liaw, K. Gering, S. Sazhin, D. Jamison, C. Michelbacher, J. Power Sources 196 (2011) 10328–10335.
[8] J. Wang, P. Liu, J. Hicks-Garner, E. Sherman, S. Soukiazian, M. Verbrugge, H. Tataria, J. Musser, P. Finamore, J. Power Sources 196 (2011) 3942–3948.
[9] M. Ecker, J.B. Gerschler, J. Vogel, S. Käbitz, F. Hust, P. Dechent, D.U. Sauer, J. Power Sources 215 (2012) 248–257.
[10] K. Honkura, K. Takahashi, T. Horiba, J. Power Sources 196 (2011) 10141–10147.
[11] Y.C. Zhang, C.Y. Wang, X.D. Tang, J. Power Sources 196 (2011) 1513–1520.
[12] G.L. Plett, J. Power Sources 134 (2004) 277–292.
[13] H.F. Dai, X.Z. Wei, Z.C. Sun, J.Y. Wang, W.J. Gu, Appl. Energy 95 (2012) 227–237.
[14] C. Hu, B.D. Youn, J. Chung, Appl. Energy 92 (2012) 694–704.
[15] G.L. Plett, J. Power Sources 196 (2011) 2319–2331.
[16] A. Hande, T.A. Stuart, J. Power Sources 138 (2004) 327–339.
[17] T.A. Stuart, W. Zhu, J. Power Sources 196 (2011) 458–464.
[18] M. Dubarry, V. Svoboda, R. Hwu, B.Y. Liaw, J. Power Sources 174 (2007) 1121–1125.
[19] I. Snihir, W. Rey, E. Verbitskiy, A. Belfadhel-Ayeb, P.H.L. Notten, J. Power Sources 159 (2006) 1484–1487.
[20] J.H. Holland, Adaptation in Natural and Artificial Systems: An Introductory Analysis with Applications to Biology, Control, and Artificial Intelligence, The MIT Press, Massachusetts, 1992.